

Periodic modulation effect on self-trapping of two weakly coupled Bose-Einstein condensates

Guan-Fang Wang,^{1,2} Li-Bin Fu,¹ and Jie Liu¹¹*Institute of Applied Physics and Computational Mathematics, P.O. Box 8009 (28), 100088 Beijing, China*²*Institute of Physical Science and Technology, Lanzhou University, 730000 Lanzhou, China*

(Received 23 September 2005; published 20 January 2006)

With phase space analysis approach, we investigate the self-trapping phenomenon for two weakly coupled Bose-Einstein condensates (BECs) in a symmetric double well potential. We identify two kinds of self-trapping by their different relative phase behavior. By applying a periodic modulation on the energy bias of the system we find that the self-trapping can be controlled, in other words, the transition parameters can be adjusted effectively by the periodic modulation. Analytic expressions for the dependence of the transition parameters on the modulation parameters are derived for high- and low-frequency modulations. For an intermediate-frequency modulation, we find the resonance between the periodic modulation and nonlinear Rabi oscillation dramatically affect the tunneling dynamics and demonstrate many phenomena. Finally, we study the effects of many-body quantum fluctuation on the self-trapping and discuss the possible experimental realization.

DOI: 10.1103/PhysRevA.73.013619

PACS number(s): 03.75.Kk, 05.45.-a, 42.50.Vk

I. INTRODUCTION

The double-well system is a paradigm model used to demonstrate quantum tunneling properties [1]. The realization of dilute Bose degenerate gas in 1995 provides an opportunity to revisit the old topics [2,3]. Here, the tunneling of Bose-Einstein condensates (BECs) differs from the traditional quantum tunneling mentioned above in two essential aspects: system scale is macroscopic ($>10 \mu\text{m}$), and more importantly, a BEC is a many-body system where the interaction between atoms plays an important role. A natural question arises, how does the interaction between the condensed atoms affect the quantum tunneling dynamics in the double-well system? This problem has attracted much theoretical attention over the past few years [4] and the recent realization of the BECs in the optical trap of a double-well configuration has brought a new research surge [5,6].

Among many findings, self-trapping is the most interesting one [7–10]. The BEC atoms in a symmetric double-well potential may show highly asymmetric distribution as if most atoms are trapped in one well, even under a repulsive interaction between the degenerate atoms. Recently, this somehow counterintuition phenomenon has been observed in experiment [6].

In this paper, we study this phenomenon with the phase space analysis approach. We emphasize the influence of a periodic modulation applied on the energy bias of the system. We find that an external ac field with high or low frequency can effectively modulate the transition parameters of the self-trapping. For a field with an intermediate frequency, we find the BECs alternate between a self-trapping regime and non-self-trapping regime with increasing atomic interaction parameter. This fact is attributed to chaos in phase space induced by the resonance between the periodic modulation and the nonlinear Rabi oscillation. Furthermore, we consider the effects of many-body quantum fluctuation on the self-trapping and find that the quantum fluctuation may dramatically influence the self-trapping phenomenon. Especially in the case of the intermediate frequency, we show that the

alternate phenomenon does not appear because there is no chaos in a full-quantum description.

The paper is organized as follows. Self-trapping phenomenon for two weakly coupled BECs is introduced and analyzed with the phase space approach in Sec. II. Section III discusses the periodic modulation for three cases: high frequency, low frequency, and a strong resonating region, respectively. After demonstrating the influence of quantum fluctuation in Sec. IV, we give our conclusion and discuss the experimental realization in Sec. V. The acknowledgment is in the final part.

II. SELF-TRAPPING IN TWO WEAKLY COUPLED BECS

We first study the dynamics of the degenerate Bose gas within a mean-field framework where the number of atoms is supposed to be infinity and the quantum fluctuation is negligible. The order parameter is then approximated by a wave function representing the density distribution of the atoms. For a double-well system, the wave function can be expressed as the superposition of individual wave functions in each well. The coefficients in the expansion will satisfy the following two-mode Gross-Pitaevskii equation (GPE) [7]:

$$i \frac{d}{dt} \begin{pmatrix} a \\ b \end{pmatrix} = H \begin{pmatrix} a \\ b \end{pmatrix}, \quad (1)$$

where a and b are the probability amplitudes of atoms in each of the two wells, respectively. The Hamiltonian is given by

$$H = \begin{pmatrix} \frac{\gamma}{2} - \frac{c}{2}(|b|^2 - |a|^2) & -\frac{v}{2} \\ -\frac{v}{2} & -\frac{\gamma}{2} + \frac{c}{2}(|b|^2 - |a|^2) \end{pmatrix}, \quad (2)$$

where v is the coupling constant between the two condensates, depending on the height of the barrier of double-well potential, γ is the energy bias between the two wells, and c is

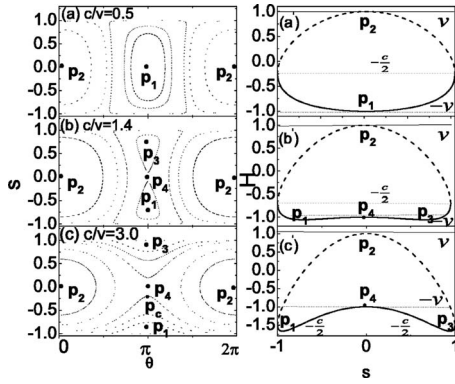


FIG. 1. Trajectories on the phase space of the Hamiltonian system (3) (left column). In the right column we plot the energy profiles for the relative phase $\theta=0$ (dashed) and $\theta=\pi$ (solid), respectively.

the nonlinear parameter describing the interaction [11–14]. The total probability is conserved and set to be 1. Our discussion focuses on the symmetric double well, meaning that $\gamma=0$.

With $a=|a|e^{i\theta_a}$, $b=|b|e^{i\theta_b}$, the Schrödinger equation can be casted into a classical Hamiltonian system by introducing the population difference $s=|b|^2-|a|^2$ and the relative phase $\theta=\theta_b-\theta_a$ [13]

$$H = \gamma s - \frac{c}{2}s^2 + v\sqrt{1-s^2}\cos\theta \quad (3)$$

with s, θ are the canonically conjugate variables of the classical Hamiltonian system.

Self-trapping refers to the phase space trajectories whose average population difference is not zero $\langle s \rangle \neq 0$. This can be well understood from the analysis on the phase space of the classical Hamiltonian system (3). Three kinds of cases will emerge with different parameters, as shown in Fig. 1.

(1) For the weak interaction, i.e., $c/v < 1$, in the phase space, there are two fixed points p_1, p_2 at $s=0, \theta=\pi$ and $s=0, \theta=0$, respectively [Fig. 1(a)]. The atoms distribution corresponding to them is in equilibrium. The trajectories around them correspond to atoms oscillation between the two wells, i.e., Josephson oscillation, and the average of population difference over the period of the oscillation is zero, i.e., $\langle s \rangle = 0$. Self-trapping phenomenon does not appear in this case.

(2) For the interaction $2 > c/v > 1$, two more fixed points appear on the line $\theta=\pi$ denoted by p_3, p_4 . Among them, p_1, p_3 are stable but p_4 is the unstable saddle point [Fig. 1(b)]. They locate at $s=-k_1, k_1, 0$, respectively, with $k_1 = \sqrt{1-(v/c)^2}$. Obviously for fixed points p_1, p_3 atoms distributions are not in equilibrium. The average of population difference about the trajectories around them is nonzero, i.e., $\langle s \rangle \neq 0$. It indicates that atoms are self-trapped in one well. Because in this case both population difference s and the relative phase θ oscillate around fixed points, we denote it as oscillating-phase-type self-trapping.

(3) With a stronger interaction, i.e., $c/v > 2$, new trajectories emerge, for example, the trajectory across point p_c [Fig. 1(c)]. For these trajectories, s changes with time only in the

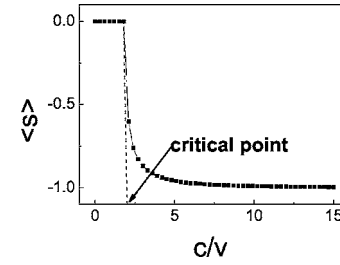


FIG. 2. The average of population difference versus the parameter c/v when the trajectory $s=-1, \theta=0$ evolves with time.

region of $[-1, 0]$ or $[0, 1]$, while the relative phase θ varies with time monotonously. Obviously $\langle s \rangle \neq 0$, atoms are self-trapped in one well, called running-phase-type self-trapping, as predicted in Refs [4,7,8,15] and observed in experiment [6].

The above changes on the topological structure of the phase space are associated with the change in the energy profile. With the relative phase being zero or π , the energy depending on the population difference s can be derived from Eq. (3) and plotted in the right column of Fig. 1 for varied parameters. The transition from case (1) to case (2) corresponds to the bifurcation of the energy profile of $\theta=\pi$: The energy curve of the single minimum bifurcates into the curve of two minima. The low limit of the energy profile with $\theta=0$ is $-c/2$, and the energy of the saddle point p_4 is $-v$, which is the local maximum of the energy profile with $\theta=\pi$. The transition from case (2) to case (3) is indicated by the overlap of the energy regime of the two profiles. In this case the trajectory originated from $s=-1, \theta=0$ cannot cross the energy hill peaked by the saddle point. The motion will be confined in the lower half of phase plane, corresponding to the running-phase-type self-trapping.

From the above analysis on the energy profile we can obtain a general criterion for the self-trapping trajectories, that is $H(s, \theta) < -v$. With the help of it, the transition parameters of self-trapping for the trajectory with arbitrary initial value can be found. For example, in the situation of recent experiment [6] $s=0.5, \theta=0$, the $c/v=15.0$ is the critical point for the transition to the running-phase-type self-trapping. For the state of initial condition $s=-1, \theta=0$ the transition parameter is $c/v=2.0$ in our analysis, agrees with our numerical simulations as shown in Fig. 2. The scaling law near the transition point shows a logarithmic singularity.

III. PERIODIC MODULATION OF SELF-TRAPPING

Generally, we can control the behavior of a system by applying a periodic modulation. For example, the tunneling dynamics can be controlled through adjusting the modulation parameters for the linear case [16–19]. In this section, we will discuss how a periodic modulation affects the nonlinear self-trapping. Without losing generality, we assume that the modulation is applied on the energy bias with amplitude A and frequency ω , i.e., $\gamma=A \sin \omega t$. Then the nonlinear GPE still can be mapped into the time-dependent Hamiltonian (3). We then can investigate the global property of the trajectory-

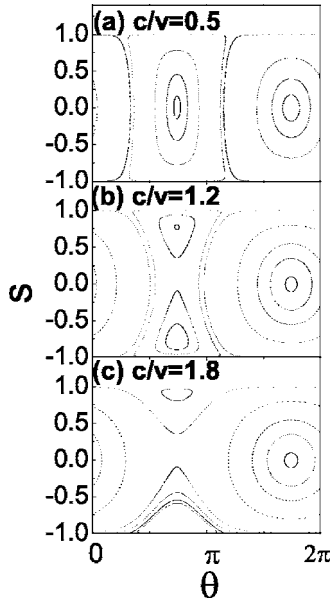


FIG. 3. Phase space of the Hamiltonian system (3) with $\gamma = A \sin \omega t$ at $\omega=100, A/\omega=1.0$, obtained by stroboscopic plotting the trajectories with period $2\pi/\omega$.

ries through phase space analysis as in the above section. Differently, in this case, the phase space of the time-dependent Hamiltonian (or Poincaré section) is drawn by stroboscopic plotting of the trajectories at the moment of integer multiple times of the modulation period, i.e., $2\pi/\omega$. We will consider the following three typical cases according to different modulation frequency regimes.

A. High-frequency modulation ($\omega \gg v$)

When a high-frequency modulation is applied to the system, two kinds of self-trapping, i.e., oscillating or running phase, still exist as shown in Fig. 3. Here the phase space is the Poincaré section of the trajectories at the moment of integer multiple times of the modulation period. Compared with Fig. 1, the fixed points are shifted to the left. This is because the phase space depends on the time moment when the Poincaré section is made. For different time moments, the topological structure of the Poincaré section remains consistent which guarantees the validity of our observation. Moreover, we find that the critical interaction parameter for the self-trapping occurrence changes dramatically with the periodic modulation. Figure 4(a), taking the trajectory $s=-1, \theta=0$ for an example, shows that the critical interaction is about 1.531 at $\omega=100, A/\omega=1.0, v=1.0$. Figure 4(b) shows the phase diagram for the transition to the self-trapping. It says that the critical values c/v depend on the modulation parameters similar to the way the Bessel function $J_0(A/\omega)$ does.

The above observation can be understood as follows. Using the high-frequency approximation, the time-dependent system (1) is equivalent to a stationary one. Let us make the transformation $a = e^{i(A/2\omega)\cos \omega t} a', b = e^{-i(A/2\omega)\cos \omega t} b'$. Then we can obtain the following Schrödinger equation:

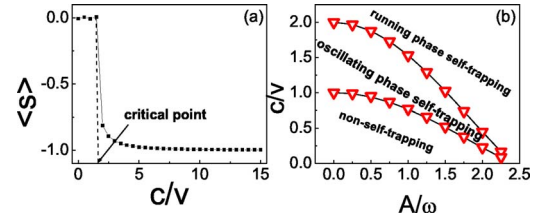


FIG. 4. (Color online) (a) The average of population difference vies parameter c/v when the trajectory $s=-1, \theta=0$ evolves with time at $\omega=100, A/\omega=1.0$. (b) Transition phase diagram for the occurrence of the self-trapping. The triangle describes the case at $\omega=100$. The line describes $J_0(A/\omega)$ (lower line) and $2J_0(A/\omega)$ (upper one).

$$i \frac{da'}{dt} = -\frac{c}{2}(|b'|^2 - |a'|^2)a' - \frac{v}{2}e^{i(A/\omega)\cos \omega t} b'. \quad (4)$$

$$i \frac{db'}{dt} = \frac{c}{2}(|b'|^2 - |a'|^2)b' - \frac{v}{2}e^{i(A/\omega)\cos \omega t} a'. \quad (5)$$

Using the formula

$$e^{\pm iz \cos \omega t} = \sum_{n=-\infty}^{\infty} J_n(z)(\pm i)^n e^{\pm in\omega t}, \quad (6)$$

where $J_n(z)$ is the Bessel function of n th order, and considering the contribution of those higher order Bessel function to the integrals can be neglected [18,20], the effective coupling constant becomes $v' = vJ_0(A/\omega)$.

Immediately, we see that the critical values are $c/v = J_0(A/\omega)$ for the oscillating phase self-trapping and $c/v = 2J_0(A/\omega)$ for the running phase self-trapping based on the results in Sec. II. This result is consistent with the numerical calculation.

B. Low-frequency modulation ($\omega \ll v$)

For this case, it is not important to identify the two kinds of self-trapping. We suppose initially all particles confined in one well with the relative phase of π , i.e., $s=-1, \theta=\pi$. Then for given parameters we check if the trajectory is self-trapped, i.e., $\langle s \rangle \neq 0$. We find that the self-trapping still occurs for some regime of parameters, as shown in Fig. 5(a). There, we see, above a critical value of interaction which is a function of modulation amplitude and the energy gap, the average population difference jumps from an irregular oscillation to a constant ($\langle s \rangle = -1$, self-trapping regime).

To see what happened before and after the transition, we plot the phase space of the system with γ changing slowly, see Fig. 6. Below the critical point, e.g., $c/v=13.5$, the fixed point p_1 (where we started from) moves up smoothly, at a certain γ_c , it collides with another fixed point p_4 and gives birth to a new trajectory. Above the critical point, e.g., $c/v=13.6$, the trajectory p_1 moves along the line $\theta=\pi$ up and down smoothly, having no chance to collide with other fixed point. For the large c case, the shift of our trajectory away from the bottom line ($s=-1$) is small that the time average of the population difference is approximately -1 .

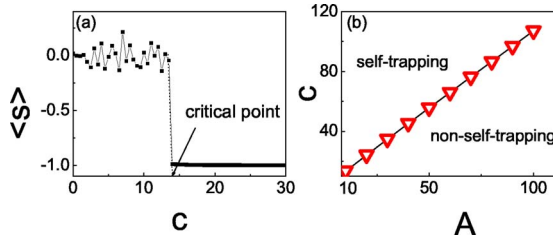


FIG. 5. (Color online) (a) The average of population difference varies the interaction parameter at $\omega=0.01, A=10, v=1.0$. (b) The relationship between the critical values of c and A when ω is extremely small at $v=1.0$. The triangle describes the situation at $\omega=0.01$. The line describes the theoretical prediction $c=(A^{2/3}+v^{2/3})^{3/2}$.

The singularity point γ_c where two fixed points collide leading to the topological change on phase space depends on the modulation amplitude but has little relation to its frequency. Our theoretical deduction gives $\gamma_c = \pm(c^{2/3} - v^{2/3})^{3/2}$ [13]. When the modulation frequency is very small, the parameter γ varies adiabatically with time $\dot{\gamma} = A\omega \cos \omega t \ll v$. If amplitude A does not exceed the critical values, atoms should be self-trapped. This gives the condition $c > (A^{2/3} + v^{2/3})^{3/2}$ for self-trapping, which agrees with the numerical result shown in Fig. 5(b). Below the critical point, the collision between the two fixed points implies the occurrence of instability, which may lead to the irregular oscillation of the average population difference as is seen in Fig. 5(a).

C. Strong resonating region ($\omega \approx v$)

For this case, the situation is complicated. Due to the strong resonance between the nonlinear Rabi oscillation and the periodic modulation, chaos appears as shown in the phase space plotting in Fig. 7, where the scattered points denote the chaotic trajectories forming a chaotic sea [21]. Inside the chaotic sea there are stable islands corresponding to the self-trapping trajectory. We find that with the increase

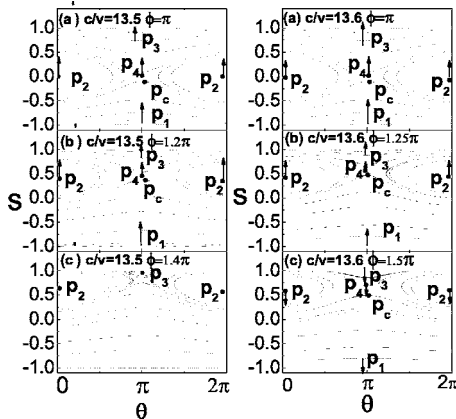


FIG. 6. Evolution of the phase space motions of the Hamiltonian system (3) with $\gamma=A \sin \omega t$ at $A=10, c/v=13.5$ (left column) and $A=10, c/v=13.6$ (right column) as γ changes adiabatically. The arrows refer to the moving direction of the fixed points as ϕ increases, i.e., γ changes adiabatically, where $\phi = \omega t$.

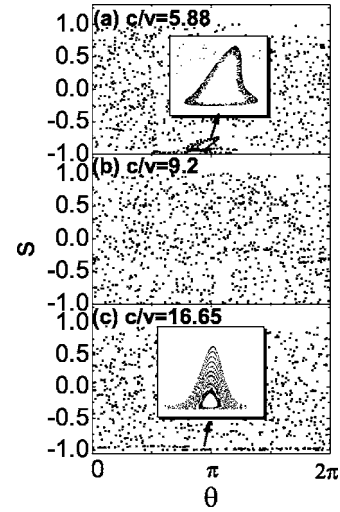


FIG. 7. Phase space of the Hamiltonian system (3) with $\gamma = A \sin \omega t$ at $\omega=2.0$, obtained by stroboscopic plotting the trajectories with period $2\pi/\omega$. (a) describes the situation at $c=5.88$, (b) at $c=9.2$, and (c) at $c=16.65$, respectively. The inset is a magnified portion.

of the interaction parameter, the stable islands appear alternately. Figure 8 describes this alternation with $\text{sgn}=1$ standing for self-trapping and $\text{sgn}=0$ for non-self-trapping when the interaction parameter varies continuously. The mutations are the transition parameters. Analytic expression for the dependence of the transition parameters on the modulation parameters cannot be found.

IV. THE EFFECT OF QUANTUM FLUCTUATION

In the above discussions on the self-trapping, our framework is the mean-field treatment with the assumption that the number of particle is infinity. However, in practical experiment, the particle number is finite and we want to know how the quantum fluctuation caused by finite number of atoms affects the self-trapping. With this motivation we investigate following second quantized Hamiltonian which is the quantum counterpart of our mean-field system (1):

$$H = -\frac{\gamma}{2}(a^\dagger a - b^\dagger b) - \frac{c}{2N}(a^\dagger a^\dagger a a + b^\dagger b^\dagger b b) + \frac{v}{2}(a^\dagger b + b^\dagger a), \tag{7}$$

where γ, c, v are the energy bias between the two modes, the interaction between atoms, and the coupling between the

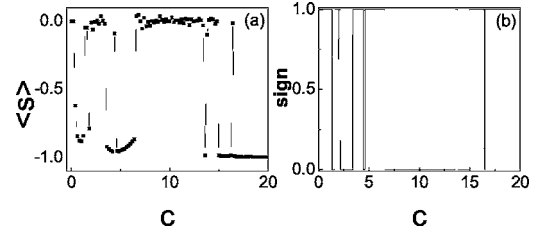


FIG. 8. (a) The average of population difference varies the interaction parameter at $\omega=2.0, A=10, v=1.0$. (b) Critical values of c for occurrence of self-trapping shows the complicated behavior at $v=1.0, \omega=2.0, A=10$. See the text for detailed explanation.

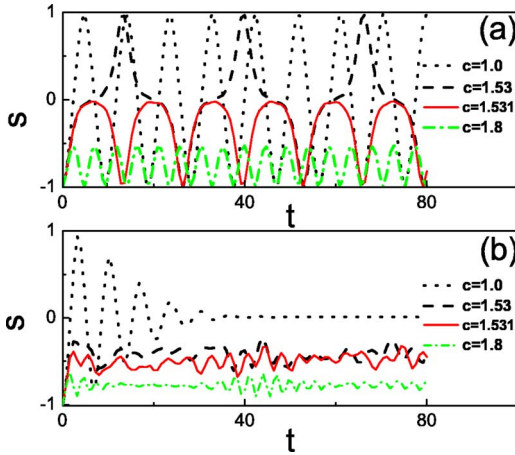


FIG. 9. (Color online) Evolution of population difference with time at $\omega=100, A/\omega=1.0, v=1.0$. (a) is mean-field results. (b) is full-quantum results.

modes, respectively. a^\dagger, b^\dagger (a, b) are creating (annihilating) boson operators. N is the total number of atoms. Its matrix elements are obtained in the representation of Fock states $|n, N-n\rangle$. $H_{n,n} = -(\gamma/2)(2n-N) - (c/2N)(2n^2 + N^2 - 2Nn - N)$, $H_{n,n-1} = H_{n-1,n} = (v/2)\sqrt{n(N-n+1)}$. Corresponding to the mean-field $s = -1$ our initial state in the full quantum framework is $|0, N\rangle$. We then can solve the corresponding Schrödinger equation $i(d/dt)a_n = H_{n,n-1}a_{n-1} + H_{n,n}a_n + H_{n,n+1}a_{n+1}$ with Runge-Kutta method, and trace the time evolution of population difference $s = \sum [|a_n|^2(N-2n)/N]$ where a_n is the amplitude of Fock state $|n, N-n\rangle$. Our main results are that, for the cases of high- or low-frequency modulation, the self-trapping effect can still be observed in full-quantum description, i.e., with increasing the interaction parameter, the quantum average population will transition from symmetric distribution to asymmetric distribution. However, different from the mean-field case, the transition here is smooth or continuous, no scaling law or singularity is observed. For the case of intermediate modulation, because the quantum effect dramatically suppress the classical chaos, and consequently the alternation phenomenon observed in the mean-field case vanishes. What we observe is a continuous transition to the self-trapping regime with increasing the interaction parameter. In the following we give a detailed presentation of our results.

For $\omega \gg v$, with increasing the interaction parameter, Fig. 9 compares the transition to self-trapping in the full-quantum treatment with that in the mean-field framework, by tracing the time evolution of population difference. It is found that, within the mean-field framework [Fig. 9(a)], there is an abrupt transition to self-trapping characterized by a logarithmic scaling law as mentioned above. However, for full-quantum calculations [Fig. 9(b)] the transition becomes smooth and no scaling law or singularity is found in this case.

For the case of $\omega \ll v$, our results are similar. As shown in Fig. 10, we find that the transition to the self-trapping regime is abrupt in the mean-field treatment [Fig. 10(a)], but smooth for the full-quantum case [Fig. 10(b)].

For the intermediate case of $\omega \approx v$, the situation is quite different. The classical chaos shown in the mean-field treat-

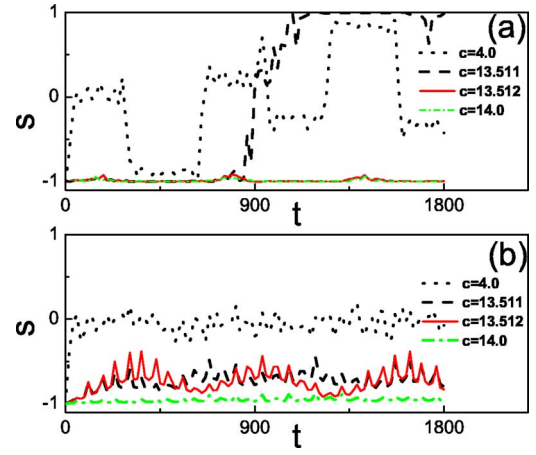


FIG. 10. (Color online) Evolution of population difference with time at $\omega=0.01, A=10, v=1.0$. (a) is mean-field results. (b) is full-quantum results. In (a) the amplitude of line $c=14.0$ is so small that it almost cannot be seen.

ment is expected to be suppressed by the quantum fluctuation and alternate phenomena observed in the mean-field case vanish, as we see in Fig. 11. With the mean-field method [Fig. 11(a)], the self-trapping effect $\langle s \rangle \neq 0$ and non-self-trapping effect $\langle s \rangle = 0$ appear alternately with increasing interaction parameter, while, in the full-quantum method [Fig. 11(b)], a continuous transition to the self-trapping regime is observed. In other words, with the increase of the interaction parameter, the BEC distribution becomes more and more self-trapped in a well.

From the above analysis, we see that in order to have a practical experiment to observe the dramatic effects of the quantum fluctuation caused by the finite number of particle, we need to choose the parameters in the regime of the occurrence of classical chaos in mean-field systems. To substantiate the above argument, we consider a concrete situation and choose parameters that are the same as in the experiment [6]. The results are demonstrated in Fig. 12. It is clearly seen for the case where the periodic modulation is absent (left column of Fig. 12) that the mean-field solution

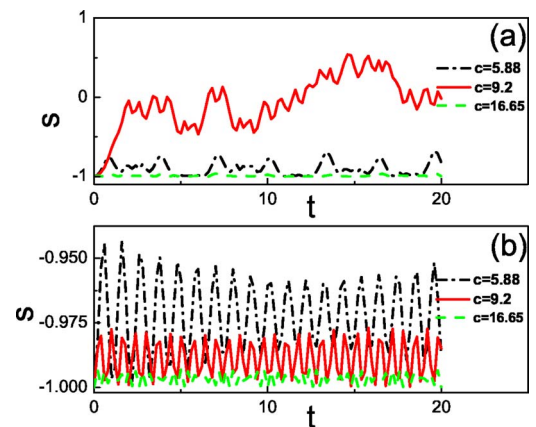


FIG. 11. (Color online) Evolution of population difference with time at $\omega=2.0, A=10, v=1.0$. (a) is mean-field results. (b) is full-quantum results.

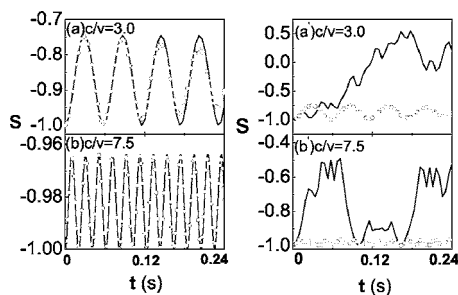


FIG. 12. Evolution of population difference with time. The lines are mean-field case. The circles are the full-quantum case. (a) and (b) are absence of the modulation. (a') and (b') are presence of the modulation with $\omega=2.0, A=10$. In (a) and (a'), $N=200$ for full-quantum case. In (b) and (b'), $N=500$ for it.

follows the quantum solution for a long time duration up to 24 ms and no significant difference is found in this case. In the above simulation, the number of the total atoms is chosen as only 200 or 500 due to the limitation of our computer capacity, which is less than 1000 of the practical experiment. However, these calculations clearly show a tendency that the larger the number of atoms, the better the correspondence between the mean-field solution and quantum solution. So we can predict a still better correspondence for the case $N=1000$. On the other hand, as chaos appears in the presence of the periodic modulation, the quantum fluctuation become huge. Caution is advised with the results from the mean-field approximation, which may be far far from the real situation as shown in the right column of Fig. 12. The above conclusion can be extended to the case of larger atom number $N=1000$ in the experimental situation [6].

V. CONCLUSIONS AND DISCUSSIONS

In conclusion, we have investigated the periodic modulation effect on the self-trapping of two weakly coupled Bose-

Einstein condensates in a symmetric double well potential both numerically and analytically. It is shown that the tunneling dynamics in this system can be controlled and the transition parameters of the self-trapping can be adjusted by applying an external periodic field. We also study the many-body quantum fluctuation effect on the self-trapping and discuss the correspondence between the mean-field solution and the full-quantum solution.

Experimentally, BEC in optical double well system can be generated by coherently splitting BEC into a double-well potential generated by two laser beams. The energy offset can be periodically modulated by adjusting the intensity of the two laser beams [5,6]. The second possible physical system that can be used to realize our model is the tunneling between the internal state of BEC as in ^{87}Rb [22,23]. There, two internal states are separated by the relatively large hyperfine energy, but in the presence of a near-resonant coupling field the states appear to be nearly degenerate. The energy bias can be adjusted by the detuning of the lasers from resonance. Our theory predicts the periodic modulation on the energy bias will dramatically affect the tunneling dynamics and the nonlinear self-trapping. We hope our discussion will stimulate further experiments.

ACKNOWLEDGMENTS

This work was supported by National Natural Science Foundation of China (Grant No. 10474008, 10445005), Science and Technology fund of CAEP, the National Fundamental Research Programme of China under Grant No. 2005CB3724503, the National High Technology Research and Development Program of China (863 Program) international cooperation program under Grant No. 2004AA1Z1220. We sincerely thank professors Biao Wu, Bing-Bing Wang, Pan-Ming Fu, and Shi-Gang Chen for their valuable discussions.

-
- [1] M. Grifoni and P. Hänggi, *Phys. Rep.* **304**, 229 (1998), and references therein.
 - [2] Franco Dalfovo *et al.*, *Rev. Mod. Phys.* **71**, 463 (1999); Anthony J. Leggett, *ibid.* **73**, 307 (2001).
 - [3] M. H. Anderson *et al.*, *Science* **269**, 198 (1995); K. B. Davis *et al.*, *Phys. Rev. Lett.* **75**, 3969 (1995); C. C. Bradley *et al.*, *ibid.* **75**, 1687 (1995).
 - [4] O. Zobay and B. M. Garraway, *Phys. Rev. A* **61**, 033603 (2000); F. Kh. Abdullaev and R. A. Kraenkel, *ibid.* **62**, 023613 (2000); F. Meier and W. Zwerger, *ibid.* **64**, 033610 (2001).
 - [5] Y. Shin *et al.*, *Phys. Rev. Lett.* **92**, 050405 (2004).
 - [6] Michael Albiez *et al.*, *Phys. Rev. Lett.* **95**, 010402 (2005).
 - [7] G. J. Milburn *et al.*, *Phys. Rev. A* **55**, 4318 (1997); A. Smerzi, S. Fantoni, S. Giovanazzi, and S. R. Shenoy, *Phys. Rev. Lett.* **79**, 4950 (1997).
 - [8] S. Raghavan, A. Smerzi, and V. M. Kenkre, *Phys. Rev. A* **60**, R1787 (1999).
 - [9] S. Raghavan, A. Smerzi, S. Fantoni, and S. R. Shenoy, *Phys. Rev. A* **59**, 620 (1999).
 - [10] Sigmund Kohler and Fernando Sols, *Phys. Rev. Lett.* **89**, 060403 (2002); L. Salasnich, *Phys. Rev. A* **61**, 015601 (2000).
 - [11] Biao Wu and Qian Niu, *Phys. Rev. A* **61**, 023402 (2000).
 - [12] Li-Bin Fu, Jie Liu, and Shi Gang Chen, *Phys. Lett. A* **298**, 388 (2002).
 - [13] Jie Liu *et al.*, *Phys. Rev. A* **66**, 023404 (2002).
 - [14] Jie Liu, Biao Wu, and Qian Niu, *Phys. Rev. Lett.* **90**, 170404 (2003).
 - [15] Martin Holthaus, *Phys. Rev. A* **64**, 011601(R) (2001).
 - [16] F. Grossman and P. H. ggi, *Europhys. Lett.* **18**, 571 (1992).
 - [17] J. M. Gomez Llorente and J. Plata, *Phys. Rev. A* **45**, R6958 (1992).
 - [18] Yosuke Kayanuma, *Phys. Rev. A* **50**, 843 (1994).
 - [19] Duan Suqing, Li-Bin Fu, Jie Liu, and Xian-Geng Zhao, *Phys. Lett. A* **346**, 315 (2005).
 - [20] Yosuke Kayanuma and Yoshihiko Mizumoto, *Phys. Rev. A* **62**,

- 061401(R) (2000).
- [21] G. L. Salmond, C. A. Holmes, and G. J. Milburn, Phys. Rev. A **65**, 033623 (2002); K. W. Mahmud, H. Perry, and W. P. Reinhardt, *ibid.* **71**, 023615 (2005).
- [22] M. Jona-Lasinio *et al.*, Phys. Rev. Lett. **91**, 230406 (2003).
- [23] M. R. Mathews *et al.*, Phys. Rev. Lett. **83**, 3358 (1999).